Átomos de Rydberg y efectos colectivos

Silvia Cárdenas López

21 de Junio de 2019

Contents

Chapter 1

Rydberg atoms

An ensemble of strongly interacting particles is highly desirable for the implementation of quantum information protocols and the simulation of quantum many-body systems. For instance, by means of strongly interacting atomic systems one can realise two photon logical gates and simulate complex condensed matter systems (study thermalization or properties out of equilibrium). These systems are also interesting from the purest theoretical point of view, since the interaction among the components of the system usually contribute in a non-trivial manner to the macroscopical response of the system.

Nowadays, several examples of such strongly interacting systems are experimentally available, such as polar molecules and ions [4]. The example that concerns this thesis is a Rydberg atoms gas, whose components interact via de Van der Waals or the dipole interaction. This system has advantages over other systems presenting strong interactions, such as tunability: the selection of the state in which each atom is on can modify both strength and type of interaction between two Rydberg atoms. The interaction can be further tunned by the precense of an external electromagnetic field.

One of the most significant consequences of the strong interaction between Rydberg atoms is the dipole blockade. Heuristically, let us have a gas of Rydberg atoms interacting with light resonant to a transition from the ground state to a Rydberg state. The interatomic interactions will take out of resonance the state of the system in which two atoms are on a Rydberg state. Consequently, we can describe the system with an effective model of

two levels, one in which all the atoms are in the ground state and one in which there is an excitation shared by all the atoms.

In this chapter, we will review how the field Rydberg quantum optics has evolved during the years. An account of the experiments and theoretical studies that have steered the current research interests of the area will be given so that we can place the current thesis on context. Along with that, we will review the principal properties of Rydberg atoms. In the end we will introduce the Rydberg blockade, the phenomenon that will concern us for the rest of the thesis.

1.1 Properties of Rydberg atoms

Rydberg atoms are atoms with one higly-excited electron[1]. They feature properties with exagerated values. In Table 1.1 we give examples of the scaling of some properties with respect to the principal quantum number, as well as numerical examples for ground state and 43S of Rubidium.

Table 1.1: Scaling of different properties with the principal quantum number. Values taken from [4]

Property	Scaling	Rb ground state	Rb(43S)
Binding energy	n^{-2}	4.18 eV	8.56 meV
Orbit radius	n^2	5.63 a_0	2384.2 a_0
Lifetime	n^3	26.2 ns	42.3 μs
C_6	n^{11}	4707 au	-1.697$\times 10^{19}$au
$\langle 5p\|er\|ns\rangle$	$n^{-1.5}$	4.23 e a_0	0.0103 ea_0
$\langle np\|er\|(n+1)s\rangle$	n^2	-	1069 e a_0

In Table 1.1 we can see that the size of the electron orbit scales as n^2. From the numerical valus given in the same table we can conclude that Rydberg atoms are gigantic when compared to atoms in the ground state.This, in turn, can be used to intuitively explain the scaling of other properties,

[1]In order to keep things simple, during this thesis we will asume that we are talking about alkaline atoms. That is, atoms with just one valence electron.

such as the strong interaction with enviroment. An electron on a Rydberg state is loosely tied to the positive core, making the system highly sensitive to external perturbations, such as electromagnetic fields and other atoms.

We can also understand the scaling of the lifetime in this way: the overlap between the wavefunctions associated with the ground state and a Rydberg state is small, so Rydberg atoms decay slowly. From the numerical examples in the table we can see that, in fact, Rydberg states are metastable when compared to the first excited states of the atom [2].

As we will later see, the valence electron of an alkaline atom on a Rydberg state is far away from the positive core.

Rydberg atoms are highly sensitive to their enviroment. That includes external electromagnetic fields and other atoms.

1.2 Early measurements of Rydberg Atoms

In 1862 J. Angström measured the spectral lines of hydrogen. In 1890 R. Rydberg gave a formula to describe the spectral lines of an atom with a single valence electron. His formula predicted that the energies of the hydrogen atom are

$$E_n = \frac{-R_H}{n^2} \tag{1.1}$$

where R_H is Rydberg's constant, and n is, in modern terms, the principal quantum number.

High-precision light sources were not available back then, making thus impossible the controlled excitation of atom to high energy states. The existence of such high energy states could only be apreciated in the nature. For instance, in 1965, astronomers detected microwave radiation coming from Orion that was evidence of the transition $n_{110} \rightarrow n_{109}$ of hydrogen atoms [3]. Rydberg states were also observable in plasmas on Earth **CITE?**.

CHECK Nonlinear quantum optics mediated by Rydberg

[2] One might argue that, due to the strong electric dipole moment between adjacent Rydberg states, fast spontaneous decay to other high energy states. This process is hindered by the small number of vacuum modes in the microwave and terahertz regions [8].

1.3 Experiments with light: Non-linear optics

With the construction of of a narrowband tunnable dye laser in 1972, precise excitation of atoms became available. This allowed to study the energetic structure of higly excited states of different atoms ([1],[10]).

Rydberg atoms couple strongly to microwave radiation. This was used by Serge Haroche to make a quantum non-demolition measurement of a photon in a cavity in 1999 [2] .

1.4 Experimental Techniques

1.4.1 Excitation

Nowadays, excitation to Rydberg states are implemented via a multi-photon scheme. If we were to use a single photon, this would be in the ultraviolet region. Instead, two or more photons excitations use infrared or visible photons.

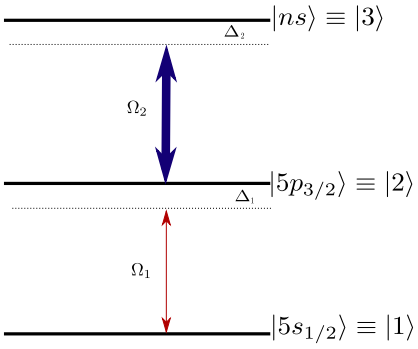

Figure 1.1

1.4.2 Detection

One can ionize a Rydberg atom by applying a sufficiently strong static electric field. This offers a procedure to measure the Rydberg population, since after ionizing one just needs to measure the number of outgoing ions.

1.5 Applications

1.5.1 Sensors of electromagnetic field

Due to their extreme sensibility to fields in the microwave and terahertz regions, Rydberg atoms offer a convenient platform to measure electromagnetic fields. First of all, atoms are the same everywhere and their properties do not age with time, therefore making them ideal meters.

1.5.2 Quantum optics

Photons in vacuum don't interact with each other. This presents a severe problem for applications in which we would like to implement gates between photons.

If photons are on a medium we can create effective interactions among them. Let's imagine first the case in which one photon is not able to change significantly the response of the system to a second photon. For instance, this would be the case if there is not interaction among the components of the medium. The photon then gets absorbed by an atom or molecule, but the rest of the components are still unperturbed. On the other hand, there are some media that present non-linearities at the level of few photons. That is, few photons are enough to produce a significant change in the response of the medium to incoming photons.

A staple example of a quantum system that can realise a non-linearity is a single atom. However, the atom-light coupling is not big enough to ensure that all photons will interact with the atom. One possible solution to this obstale is to introduce the atom in a cavity.

Another possible candidate for the creation of few photons non-linearities is a Rydberg medium. The principal agent in this non-linearity is the Rydberg blockade, that we discuss next.

1.6 Rydberg blockade

Due to the large electric dipole moment Rydberg atoms interact strongly with one another. There are two types of interaction

- Dipole-Dipole interaction:

$$V(R) = \frac{C_3}{R^3} \tag{1.2}$$

- vad der Waals interaction:

$$V(R) = \frac{C_6}{R^6} \tag{1.3}$$

Occurs when the two interacting atoms are in the same Rydberg state.

Let us consider two two-level atoms, as depicted in figure 1.2(a). The two levels of each atom are $|g\rangle$ and $|r\rangle$. We will suppose that $|r\rangle$ is a Rydberg state and that atoms interact through a van der Waals potential of the form $V(R) = \frac{C_6}{R^6}$ only when both atoms are on a Rydberg state. Furthermore, assume that we drive the transition $|g\rangle \rightarrow |r\rangle$ with a laser and that the process is described by the Rabi frequency Ω. The whole situation is then described by the hamiltonian:

$$\begin{aligned} H = {} & E_r \left|rg\right\rangle \left\langle rg\right| + E_r \left|gr\right\rangle \left\langle gr\right| + 2Er \left|rr\right\rangle \left\langle rr\right| + \frac{C_6}{R^6} \left|rr\right\rangle \left\langle rr\right| \\ & + \left(\Omega \left|rg\right\rangle \left\langle gg\right| + \Omega \left|gr\right\rangle \left\langle gg\right| + \text{H.c.}\right) \end{aligned} \tag{1.4}$$

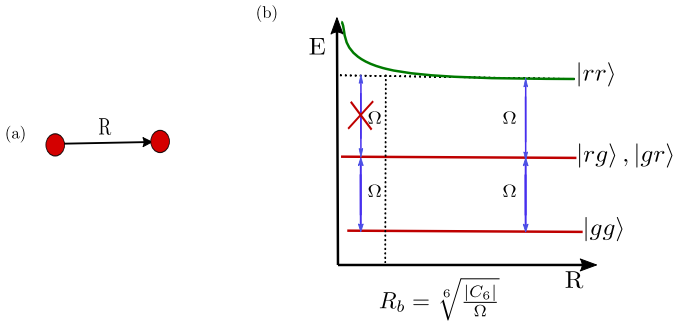

Figure 1.2

As illustrated in figure 1.2(b), only the level $|rr\rangle$ will be shifted due to the interaction. At a critical separation between atoms, R_b, excitation to the

upper level due to light will be strongly suppresed, and the system of two atoms will contain one excitation at most. The phenomenon just described here is called Rydberg blockade, and it will be a central topic in our study.

The Rydberg-Rydberg interaction was experimentally observed by broadening of spectral lines in ^{87}Rb [7] Rydberg blockaded oscillations with two atoms were observed in 2009 [11].

Chapter 2

Calculation of Rydberg Potentials

2.1 Introduction

In this section, we will review the procedure to numerically calculate Rydberg potentials. The work of this section is based on the tutorial [12].

First of all, we should clarify what do we mean by a Rydberg potential. Let us think that we have two alkaline atoms. As it was stated in the last chapter, when both atoms are on a Rydberg state, the interaction among them is strong. As a result, the energy of the state in which both atoms are on a Rydberg state is a function of R, the separation between the atoms[1]. See figure (1.2) for example: the energy of the level $|rr\rangle$ is a function $E_{rr}(R)$. This function is what we will call Rydberg potential. The dependence on R of E_{rr} is what ultimately origins the blockade. In order to fully characterize the two-body blockade, the fist natural step is to characterize the potential.

Our objetive in this section is then to calculate the functions $E_{r_1 r_2}(R)$ (we generalize to the case in which the two atoms can be in different Rydberg states). The subindex r_i contains the quantum numbers that completely describe the state of the atom: $r_i \equiv (n_i, \ell_i, j_i, m_{j_i})$.

[1]During the whole thesis, we will assume that the motion of the atoms is frozen. That is, that R is not a degree of freedom of the system, but a mere parameter that is fixed at the beginning and doesn't change through the evolution of the system.

The steps that we will follow to calculate $E_{r_1 r_2}(R)$ are:

- Step 1: Calculation of wavefunctions that describe Rydberg states on an alkaline atom
- Step 2: Selection of significant basis
- Step 3: Calculation of the energy via the Rayleigh Ritz method for different R.

2.2 Step 1: Wavefunctions of alkaline atoms

The hamiltonian describing a system of two atoms is

$$\begin{aligned} H &= H_1 \otimes \mathbf{1} + \mathbf{1} \otimes H_2 + \frac{\vec{d_1} \cdot \vec{d_2} - 3(\hat{r} \cdot \vec{d_1})(\hat{r} \cdot \vec{d_2})}{r^3} \\ &= H_0 + H_{\mathrm{dd}} \end{aligned} \tag{2.1}$$

We have only included the lowest order of electrostatic interaction between the atoms, namely the dipole-dipole interaction. In the last line we named the hamiltonian without interactions as H_0, and the dipole-dipole coupling as H_{dd}. H_i is the hamiltonian that describes the i-atom. The first step consists in finding the eigenfunctions of this hamiltonians.

Since alkaline atoms are multielectronic atoms, there is not an exact analytic solution to this problem. However, alkaline atoms are special in the sense that they have only one valence electron. This allow us to treat the atom as one electron and a positive core (composed by the nucleus and the closed electronic shells). This, in turn, allow us to describe the valence electron (and the whole atom) by a one-body wavefunction. The more excited the atom is, the more accurate this approximation is, since the valence electron will be far away from the positive core. If it is far away, effects caused by the fact that the atom has many electrons will be negligible.

With this taken into account, there are two ways in which one can obtain the wavefunctions. The first option is to propose an effective potential that describes the positive core and to numerically solve the Schrödinger equation. The second option is to use the quantum defect theory to obtain analytical

expressions that approximate the real wavefunctions. We next describe each approach and give a comparision between them.

2.2.1 Effective potential and numerical solution

The effective potential used to describe the positive core formed by the nucleus and the closed shells on an alkaline atom is [5]:

$$V(r) = -\frac{Z_{nl}(r)}{r} - \frac{\alpha_c}{2r^4}\left(1 - e^{-\left(\frac{r}{r_c}\right)^6}\right) + V_{so} \tag{2.2}$$

where

$$Z_{nl}(r) = 1 + (Z-1)e^{-a_1 r} - r(a_3 + a_4 r)e^{-a_2 r}$$

and $V_{so} = \alpha\frac{\vec{L}\cdot\vec{S}}{r^3}$ is the spin-orbit coupling.

We will refer to the potential (2.2) as Marinescu potential. The first term is a Coulomb potential. The function $Z_{nl}(r)$ seeks to model the fact that the positive core has a charge distribution. The second term takes into account that the closed shells can be deformed in the presence of the valence electron. The parameters a_i and r_c are adjusted so that the energy spectrum of potential(2.2) agrees with the measured spectrum of different alkaline atoms. The values for these parameters for some alkaline atoms can be found in [5].

Since this is a central potential, we separate the Schrödinger equation in spherical coordinates. Furthermore, we already know that the angular solution will be spherical harmonics. In order to completely know the wavefunctions and the energies of the problem we need to solve

$$\frac{d^2u}{dr^2} + 2\left(E - V_M(r) - \frac{\ell(\ell+1)}{2r^2}\right)u = 0 \tag{2.3}$$

In the last equation we have supposed $\mu = 1$, $\hbar = 1$ and $u = rR$, R being the radial part of the wavefunction.

Using the parameters for ^{87}Rb from [5] we numerically solved the equation (2.3) using the Matrix Numerov method (which is reviewed on Appendix A). We obtained the wavefunctions and energies for principal quantum number between 40 and 80, with

- $\ell = 0$,j=0.5
- $\ell = 1$,j=0.5,1.5
- $\ell = 2$,j=1.5,2.5
- $\ell = 3$,j=2.5,3.5

2.2.2 Quantum defect theory and Coulomb functions

With the quantum defect theory, an approximated solution for the Schrödinger radial equation for alkaline atoms can be obtained. This solutions are the so-called Coulomb functions:

$$\psi_{n^*l}^{(\mathrm{rad})} = \left(\frac{1}{a_0}\right)^{3/2} \frac{1}{\sqrt{(n^*)^2\Gamma(n^*+l+1)\Gamma(n^*-l)}} W_{n^*,l+1/2}\left(\frac{2r}{n^*a_0}\right) \tag{2.4}$$

where W_k, n is the Whittaker function, and Γ is the gamma function. n^* is que effective principal quantum number. This solutions are particularly accurate for big r, so they are effective to describe Rydberg atoms.

This theory also gives a formula for the atom energies:

$$E_{n\ell j} = -\frac{Ry^*}{n^{*2}} \tag{2.5}$$

Ry^* is the modified Rydberg constant $Ry^* = \frac{Ry}{1+m_e/m_{\mathrm{atom}}}$ and $Ry = 13.6eV$. The effective principal quantum number, n^*, can be parametrized as

$$n^* = n - \delta_{nlj}$$

δ_{nlj} is named the defect. It can be expressed as:

$$\delta_{nlj} = \delta_0 + \frac{\delta_2}{(n-\delta_0)^2} + \frac{\delta_4}{(n-\delta_0)^4} + ... \tag{2.6}$$

The coefficients δ_i are obtained adjusting (2.5) to the experimental transition energies. We used the coefficients δ_i reported in [13].

2.2.3 Comparison between the two approaches

In the figure 2.1 we compare 3 of the wavefunctions obtained with Numerov with the Coulomb functions and the wavefunctions given by the ARC library from Python [9].

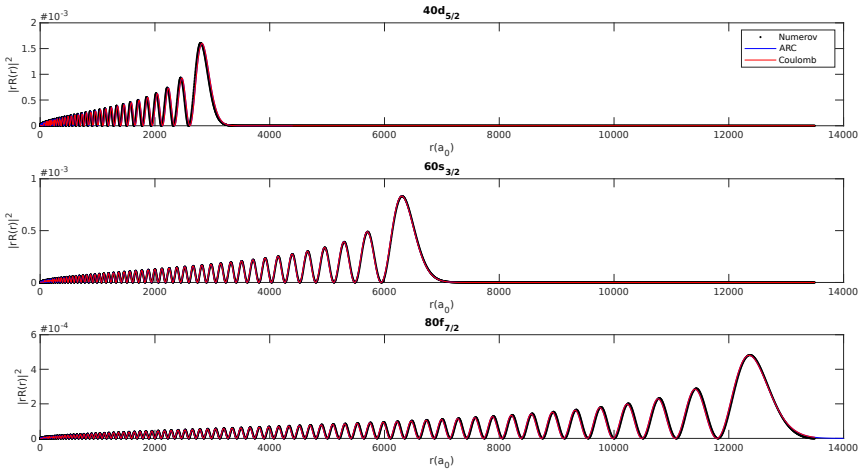

Figure 2.1: Comparison between Numerov,Coulomb and the wavefunctions obtained in ARC [9].

We see that the two methods agree with the functions from the ARC library for big r. Coulomb functions appreciably differ from the other two for small r. However, this will not represent a serious problem since we want the wavefunctions to calculate matrix elements of the dipole operator $e\vec{r}$. The most important contributions for this elements will come from the region far from the origin.

2.3 Matrix elements

Now we describe how to calculate matrix elements using pairs of the functions calculated in the last section. Let's suppouse that we form the basis of N elements

$$\mathbf{B} = \{\psi_{r_{1i}}(\vec{r}_1)\psi_{r_{2i}}(\vec{r}_2)\}_{i=1}^{N} \tag{2.7}$$

Each element of the basis is a product of a wavefunction describing atom 1, $\psi_{r_{1i}}(\vec{r}_1)$, and a wavefunction describing atom 2, $\psi_{r_{2i}}(\vec{r}_2)$ (we continue to use the notation $r_i \equiv (n_i, \ell_i, j_i, m_{j_i})$). Our objective is to calculate the matrix representation of the hamiltonian (2.1) in this basis.

We note in the first place that $H_1 \otimes \mathbf{1} + \mathbf{1} \otimes H_2$ is diagonal in this basis. These diagonal elements are the sum of the energies of the two atoms without interaction:

$$(H_1 \otimes \mathbf{1} + \mathbf{1} \otimes H_2)_{ii} = E_{r_{1i}} + E_{r_{2i}}$$

We get those energies either from the Numerov results or the formula (2.5).

In order to calculate the matrix elements of the interaction term H_{dd} we will first calculate the elements

$$\langle n\ell jm|d_q|n'\ell' j'm'\rangle$$

where d_q is the q-component of the dipolar moment on a given basis. We will use the spherical components:

$$\begin{aligned} d_0 &= d_z \\ d_{\pm 1} &= \mp \frac{d_x \pm i d_y}{\sqrt{2}} \end{aligned} \tag{2.8}$$

This will be convenient since we will be able to use Wigner-Eckart theorem.

2.3.1 Wigner-Eckart theorem

We define an irreducible tensor of range κ as a set of $2\kappa + 1$ operators such that all operators have the same transformation properties as the spherical harmonics $Y_{\kappa q}$ under a rotation of the system of coordinates. We will denote these objects as $T_{\kappa q}$.

The Wigner-Eckart theorem allows us to express the matrix elements of these objects as

$$\langle n\ell sjm_j|T_{\kappa q}|n'\ell's'j'm'_j\rangle = (-1)^{j-m_j}(nlsj||T_{\kappa 0}||n'l's'j')\begin{pmatrix} j & \kappa & j' \\ -m_j & q & m'_j \end{pmatrix} \tag{2.9}$$

$(nlsj||T_{\kappa 0}||n'l's'j')$ is the reduced matrix element. We put a zero in the subindex instead of a q to explicitly indicate that this element doesn't depend on q. The factor (...) is called 3j Wigner symbol, and it is related to Clebsch Gordan in the following way:

$$\langle j_1 j_2 m_1 m_2|j_1 j_2 JM\rangle = (-1)^{j_1-j_2-M}\sqrt{2j+1}\begin{pmatrix} j_1 & j_2 & J \\ m_1 & m_2 & -M \end{pmatrix}$$

The spherical components of the dipole moment form a tensor with range one because we can express them as

$$d_q = er\sqrt{\frac{4\pi}{3}}Y_{1q} \tag{2.10}$$

This means we can apply Wigner-Eckart theorem and the elements we need to calculate will look like (2.9) with $\kappa = 1$. Thus we only need to compute the reduced matrix element $(lsj||d_q||l's'j')$. According to [**?**], this quantity is:

$$(nlsj||d_q||n'l's'j') = (-1)^{\ell+s+j'+1}(nl||d_q||nl')\sqrt{(2j+1)(2j'+1)}\begin{Bmatrix} l & j & s \\ j' & l' & 1 \end{Bmatrix} \tag{2.11}$$

where {...} is the 6j Wigner symbol (that can be defined in term s of 3j Wigner symbols). $(l||d_q||l')$ can be separated in an angular and a radial part:

$$\begin{aligned}(nl||d_q||n'l') &= \int_0^\infty dr R_{n\ell}(r)(er)R_{n'\ell'}(r)r^2(nl||\sqrt{\frac{4\pi}{3}}Y_{1q}||n'l') \\ &= (-1)^\ell\sqrt{(2\ell+1)(2\ell'+1)}\begin{pmatrix} l & 1 & l' \\ 0 & 0 & 0 \end{pmatrix}\int_0^\infty dr R_{n\ell}(r)(er)R_{n'\ell'}(r)r^2\end{aligned}$$

In summary, the q component of $\vec{d}$ will have matrix elements of the form:

$$\langle n\ell jm|d_q|n'\ell' j'm'\rangle = \mu(n,\ell,j,n',\ell',j')C^q(j,m_j,j',m'_j)$$
$$C^q = (-1)^{j'-1+m_j}\begin{pmatrix} j' & 1 & j \\ m'_j & q & -m_j \end{pmatrix}$$
$$\mu = (-1)^{j'+1+s}\sqrt{(2\ell+1)(2\ell'+1)(2j+1)(2j'+1)}\begin{pmatrix} l & 1 & l' \\ 0 & 0 & 0 \end{pmatrix}$$
$$\times \begin{Bmatrix} j & 1 & j' \\ \ell' & s & \ell \end{Bmatrix}\int_0^\infty dr R_{n\ell}(r)(er)R_{n'\ell'}(r)r^2 \tag{2.12}$$

On figure 2.2 we graph the radial part of the matrix element (μ) vs the difference of principal quantum numbers of the states involved.

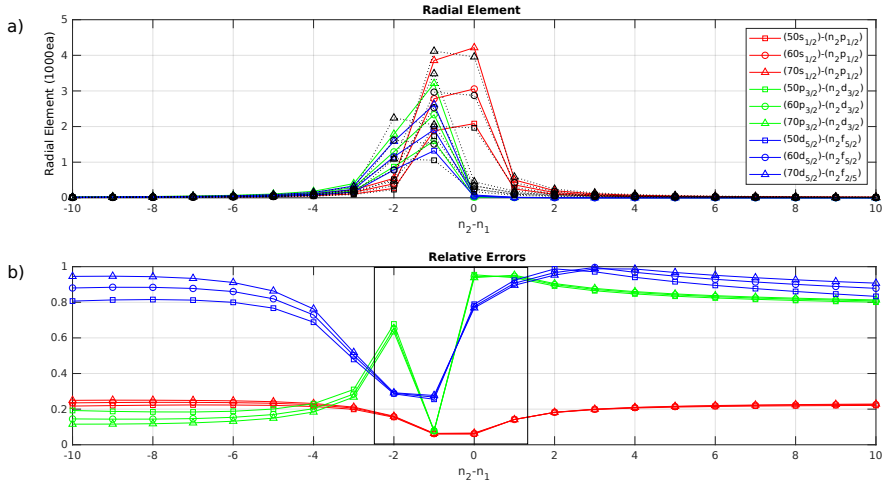

Figure 2.2: (a)Radial matrix element between some states. Data in color corresponds to the results obtained with Coulomb functions. Data in black corresponds to the results with Numerov.(b)Relative difference between color and black data.

The results obtained with Coulomb and Numerov have the same qualitative behavior: both go to zero if the difference between principal quantum numbers increases. We can understand this intuitively. If the two quantum numbers are not alike it means that the overlap between the corresponding

wavefunctions will not be big[2]. As we shall see in next section, this observation is useful as a criteria to identify states that will not be relevant for the calculation of a potential.

However, if we quantitatively compare both sets we obtain that the difference is important in some regions and for some angular momenta (figure 2.2(b)). The relative error for the bigger and most relevant matrix elements are enclosed by the black rectangle.

2.4 Step 2: Relevant basis and symmetries

2.4.1 Energy criterion

Let us suppouse that we are calculating the potential for the pair of states $\psi_{n_1,\ell_1,j_1,m_{j_1}}$ and $\psi_{n_2,\ell_2,j_2,m_{j_2}}$ and we have chosen a basis like (2.7) to build the matrix representation of hamiltonian (2.1). Elements not belonging to the diagonal will be caused by H_{dd}, and will contain products of the dipole matrix elements analysed in last section. As we have seen on last section, the dipole matrix element $\langle n\ell jm|d_q|n'\ell' j'm'\rangle$ tends to zero as the difference $|n-n'|$ increases. This means that the most relevant states to include on the basis are $\psi_{n_3,\ell_3,j_3,m_{j_3}}(\vec{r}_1)\psi_{n_4,\ell_4,j_4,m_{j_4}}(\vec{r}_2)$ where n_3 is close to n_1 and n_4 is close to n_2 or viseversa (states that don't have such quantum numers will couple weakly to the state of interest and hence will not contribute to the potential). If the last condition is fulfilled it means that $E_{n_1\ell_1,j_1} + E_{n_2\ell_2,j_2} \simeq E_{n_3\ell_3,j_3} + E_{n_4\ell_4,j_4}$, so the first criterion to reduce the basis can be restated as:

Condition 1:$\psi_{n_3,\ell_3,j_3,m_{j_3}}(\vec{r}_1)\psi_{n_4,\ell_4,j_4,m_{j_4}}(\vec{r}_2)$ will be included on the relevant basis if $|E - E_{34}| < \Delta$, where E is the energy of the state of interest and E_{34} is the energy of state under consideration. Δ is a pre-established number. The bigger it is, the more states will be included on the basis, and the more exact the obtained potential will be.

[2]Look at the figure (2.1). The biggest contribution for the radial integral that appears in (2.12) will come from the biggest hump of each wavefunction. If the principal quantum numbers are alike it means that the humps have a big overlap. Conversely, if they are too different, the humps will have a negligible overlap and the integral's value will be small.

2.4.2 Symmetries

We can use the symmetries of an homonuclear molecule to further decrease the size of the relevant basis without decreasing the precision of the results. The key argument is that two states with different symmetry properties, namely $|\psi_1\rangle$ and $|\psi_2\rangle$, will not be coupled by the hamiltonian (that is $\langle\psi_1|H|\psi_2\rangle = 0$). This induces a block diagonal structure on the matrix associated to the hamiltonian, where each block corresponds to states with particular symmetry properties. In order to obtain the potential of a chosen state we only need to include states with the same symmetry properties on the basis.

The symmetry group of an homonuclear system is $D_{\infty h}$. The elements of this group are:

- C_ϕ: Rotation by the angle ϕ about the molecule axis.
- iC_2': Reflection across any plane that contains the molecule axis.

These symmetries have an associated conserved quantity. If we align the molecule axis to $\hat{z}$, then the conserved quantity associated to C_ϕ is the component along $\hat{z}$ of the sum of angular momentum. This means

$$\langle n_1\ell_1 s_1 j_1 m_{j_1} n_2\ell_2 s_2 j_2 m_{j_2}|H|n_1'\ell_1' s_1' j_1' m_{j_1}' n_2'\ell_2' s_2' j_2' m_{j_2}'\rangle \neq 0 \Leftrightarrow m_{j_1}+m_{j_2} = m_{j_1}'+m_{j_2}' \tag{2.13}$$

We can exploit the iC_2' symmetry by choosing the xz plane (so the symmetry transformation is $\vec{y} \to -\vec{y}$) and changing to the basis:

$$|\psi\rangle_{+/-} = \frac{1}{\sqrt{2}}\left(|n_1\ell_1 s_1 j_1 m_{j_1} n_2\ell_2 s_2 j_2 m_{j_2}\rangle + d(-1)^{l_1+l_2+m_{j_1}+m_{j_2}-j_1-j_2}\,|n_1\ell_1 s_1 j_1 - m_{j_1} n_2\ell_2 s_2 j_2 - m_{j_2}\rangle\right) \tag{2.14}$$

where $d = \pm 1$. The hamiltonian will not couple states + with states -. Note that this state only has well defined total angular momentum if $m_{j_1} + m_{j_2} = 0$. This is because C_ϕ and iC_2' don't commute. For the case $m_{j_1} + m_{j_2} = 0$ we can use both symmetries, and for the case $m_{j_1} + m_{j_2} \neq 0$

we only use the rotation symmetry.

Another symmetry transformation of the system is that of inversion: $(\vec{r}_i \to -\vec{r}_i, \vec{R} \to -\vec{R})$. A symmetrized basis that can be used to explote this symmetry is:

$$|\psi\rangle_{g/u} = \frac{1}{\sqrt{2}} \left(|n_1 \ell_1 s_1 j_1 m_{j_1} n_2 \ell_2 s_2 j_2 m_{j_2}\rangle - p(-1)^{l_1+l_2} |n_2 \ell_2 s_2 j_2 m_{j_2} n_1 \ell_1 s_1 j_1 m_{j_1}\rangle \right) \tag{2.15}$$

$|\psi\rangle_{g/u}$ is said to have gerade/ungerade symmetry. $p = \pm 1$ for g/u. The hamiltonian will not couple gerade states with ungerade ones.

The last symmetry is permutation:$\vec{R} \to -\vec{R}$. The basis to exploit this symmetry is

$$|\psi\rangle_{s/a} = \frac{1}{\sqrt{2}} \left(|n_1 \ell_1 s_1 j_1 m_{j_1} n_2 \ell_2 s_2 j_2 m_{j_2}\rangle - f\, |n_2 \ell_2 s_2 j_2 m_{j_2} n_1 \ell_1 s_1 j_1 m_{j_1}\rangle \right) \tag{2.16}$$

where $f = \pm 1$ for s/a. Since we have both permutation and inversion symmetry, we can realize by looking at equations (2.15) and (2.16) that $P = (-1)^{\ell_1+\ell_2}$ is also a conserved quantity of the system.

In summary, we further reduce the size of the basis to calculate the potential associated with $\psi_{n_1,\ell_1,j_1,m_{j_1}} \psi_{n_2,\ell_2,j_2,m_{j_2}}$

- Choosing either the gerade or ungerade symmetry for the state for which we want the calculate the potential
- Calculating P and $M = m_{j_1} + m_{j_2}$
- Eliminating states from the basis that doesn't have the same P or M and symmetrizing the surviving states to match the g or u symmetry chosen for the relevant state.

All these steps amount to choose a block on the diagonal of the matrix depicted in figure 2.3

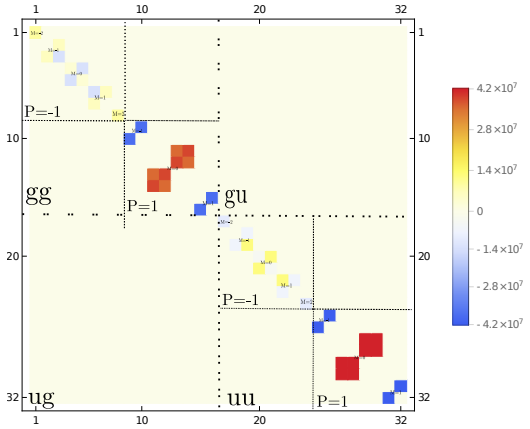

Figure 2.3: Example of the block structure induced by the symmetries of the system.

On figure 2.4 we can appreciate that the effort of taking into account the symmetries of the system pays well in the reduction of the size of the problem.

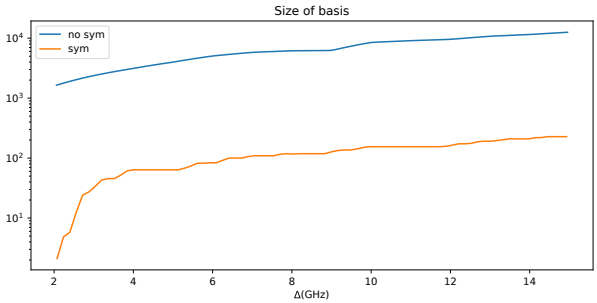

Figure 2.4: Size of the basis vs Δ with and without the use of symmetries.

2.5 Step 4: Construction of matrix and potentials

2.5.1 Symmetrized matrix elements

Now that we have the reduced basis we are ready to construct the matrix representing the hamiltonian.

To calculate the matrix elements we first have to symmetrize the states (gerade or ungerade). Alternatively, we can implement the symmetrization at the level of matrix elements. For this purpose, let's calculate $\langle\psi|d_{q_\alpha}d_{q_\beta}|\phi\rangle$ (which is the type of elements we have to calculate when building the matrix associated with H_{dd}) where $|\psi\rangle$ y$|\phi\rangle$ are states with g or u symmetry:

$$|\psi\rangle = \frac{1}{\sqrt{2}}\left(|\eta_1\eta_2\rangle - p_\psi(-1)^{l_1+l_2}\,|\eta_2\eta_1\rangle\right)$$
$$|\phi\rangle = \frac{1}{\sqrt{2}}\left(|\eta_3\eta_4\rangle - p_\phi(-1)^{l_3+l_4}\,|\eta_3\eta_4\rangle\right)$$

where $\{n_1, l_1, j_1, m_1\} \equiv \eta_1$. By a direct calculation we obtain

$$\begin{aligned}2\,\langle\psi|d_{q_\alpha}d_{q_\beta}|\phi\rangle = {} & \langle\eta_1|d_{q_\alpha}|\eta_3\rangle\,\langle\eta_2|d_{q_\beta}|\eta_4\rangle - p_\phi(-1)^{l_3+l_4}\,\langle\eta_1|d_{q_\alpha}|\eta_4\rangle\,\langle\eta_2|d_{q_\beta}|\eta_3\rangle \\ & - p_\psi(-1)^{l_1+l_2}\,\langle\eta_2|d_{q_\alpha}|\eta_3\rangle\,\langle\eta_1|d_{q_\beta}|\eta_4\rangle \\ & + p_\psi p_\phi(-1)^{l_1+l_2+l_3+l_4}\,\langle\eta_2|d_{q_\alpha}|\eta_4\rangle\,\langle\eta_1|d_{q_\beta}|\eta_3\rangle\end{aligned} \tag{2.17}$$

2.5.2 Associated matrix

As we have previously mentioned,

$$H = H_0 + H_{\mathrm{dd}}$$

H_0 is diagonal in the chosen basis. On the other hand,

$$
\begin{aligned}
H_{dd} &\equiv \frac{\vec{d_1}\cdot\vec{d_2} - 3(\hat{r}\cdot\vec{d_1})(\hat{r}\cdot\vec{d_2})}{r^3} \\
&= \frac{d_{1z}d_{2z}(1-3\cos^2\theta) - d_{1+}d_{2-} - d_{1-}d_{2+}}{r^3} \\
&- \frac{3\sin^2\theta(d_{1+}d_{2+} + d_{1-}d_{2-} - d_{1+}d_{2-} - d_{1-}d_{2+})}{2r^3} \\
&- \frac{3\sin\theta\cos\theta(d_{1-}d_{2z} - d_{1+}d_{2z} + d_{1z}d_{2-} - d_{1z}d_{2+})}{\sqrt{2}r^3}
\end{aligned}
\tag{2.18}
$$

where θ is the angle between the quantization axis and the molecular axis. The matrix elements of the each of the operators $d_{q_\alpha}d_{q_\beta}$ appearing on equation (2.18) can be calculated using the formula (2.17).

2.5.3 Potentials

We are ready to obtain the potential for a given state $\psi_{n_1,\ell_1,j_1,m_{j_1}}\psi_{n_2,\ell_2,j_2,m_{j_2}}$ for a range of separation between atoms $[r_{\min}, r_{\max}]$. For each r on that range, we build the matrix associated to the hamiltonian and diagonalize. For each r we then will have N eigenvalues and eigenvectors. For each r, we will choose the eigenvalue that matches the eigenvector with the biggest overlap to the state $\psi_{n_1,\ell_1,j_1,m_{j_1}}\psi_{n_2,\ell_2,j_2,m_{j_2}}$. The potential will be the curved formed by the selected points.

2.5.4 C_6

2.5.5 Mixing of states

Chapter 3

Two Rydberg atoms on a cavity

Having characterized the interaction between two Rydberg atoms we are ready to study the atoms in a cavity. In order to simplify things we consider only two atoms. The situation we will study is depicted in figure 3.1(b). Two ^{87}Rb atoms separated by a distance R are inside a cavity. The red laser feeds the cavity and the blue laser enters transversally to the cavity and interacts directly with the two atoms.

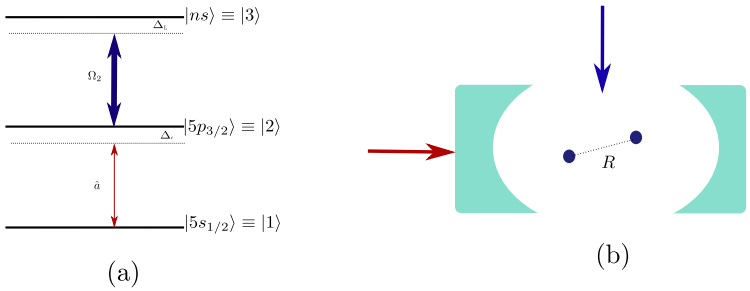

Figure 3.1: (a) Excitation scheme (b)Situation under consideration

The two lasers can excite each atom individually from the ground state $|1\rangle$ to a Rydberg state $|3\rangle$ via a two-photon transition(figure 3.1(a)), as we described in the introduction chapter. The first and second transitions are repectively mediated by the cavity and the blue laser.

Let ω_c be the frequency of the cavity and ω_L be the frequency of the blue laser. The detuning between the cavity and the transition $|1\rangle \rightarrow |2\rangle$

is $\Delta_c = \omega_{12} - \omega_c$. Likewise, the detuning between the blue laser and the transition $|2\rangle \to |3\rangle$ is $\Delta_L = \omega_{23} - \omega_L$.

The hamiltonian describing the system (in the interaction picture with respect to the cavity) is

$$\begin{aligned} H = &\sum_{im} E_i \sigma_{ii}^{(m)} + H_{dd} + \sum_m \hbar g(x_m) \left(a\sigma_{12}^{(m)} e^{i\omega_c t} + a_c^\dagger \sigma_{21}^{(m)} e^{-i\omega_c t} \right) \\ &- (\vec{d_1} + \vec{d_2}) \cdot \vec{E}_L + \hbar \left(\alpha^* a^\dagger e^{-i\omega_c t} + \alpha a e^{i\omega_c t} \right) \end{aligned} \tag{3.1}$$

The first term describes the energy of each atom (we name $\sigma_{ij}^{(m)} \equiv |i\rangle_m \langle j|_m$).The second term is the electrostatic dipole interaction between the two atoms:

$$H_{dd} = \frac{\vec{d_1} \cdot \vec{d_2} - 3(\vec{d_1} \cdot \hat{r})(\vec{d_2} \cdot \hat{r})}{R^3} \tag{3.2}$$

where $\vec{d_i}$ is the electric dipole operator of the i-th atom.

3.1 Effective model

We now deduce an effective model to describe the two atoms. The first step is to diagonalize the part of the hamiltonian that refers only to the atoms:

$$H_A = \sum_{im} E_i \sigma_{ii}^{(m)} + H_{dd} \tag{3.3}$$

This is what we have done in chapter 2. There, we learnt that the most important states to include on the basis to obtain the potential for a pair of atoms in Rydberg states, r_1 and r_2, were pair states whose energy was close to the energy $E_{r_1} + E_{r_2}$. In order to get the potentials from diagonalising (3.3) we need to enlarge our basis and include pair states where atoms are on Rydberg states different from $|3\rangle$. We take our basis to be:

$$\mathcal{B} = \{|1\rangle, |2\rangle, |3\rangle, |\beta_1\rangle, |\beta_2\rangle, ...\} \otimes \{|1\rangle, |2\rangle, |3\rangle, |\beta_1\rangle, |\beta_2\rangle, ...\}$$

where $|\beta_i\rangle$ are Rydberg states different from $|3\rangle$. In order to choose the states $|\beta_i\rangle$ to be taken into account, we use the energy and symmetries criteria

described in chapter 2. Diagonalising the matrix representation of H_A with respect to this basis gives us eigenstates of the form:

$$|\xi_L(R)\rangle = \sum_{\alpha\beta} C^L_{\alpha\beta}(R)\,|\alpha\beta\rangle \tag{3.4}$$

The composition coefficients will depend on the separation R between atoms.

First approximation

Our first approximation will consist on neglecting dipolar matrix elements between two non-Rydberg states present in the basis ($|1\rangle$ and $|2\rangle$), as well as the dipolar matrix element between a Rydberg state and a non-Rydberg one. The justification of this approximation is clear if we examine the value of the matrix element for each case. As we saw in table 1.1,

$$\begin{aligned}\langle 43S|er|44S\rangle &= 1069ea_0\\ \langle 43S|er|5P\rangle &= 0.0103ea_0\\ \langle 5P|er|5S\rangle &= 4.23ea_0\end{aligned}$$

The dipolar matrix element between two Rydberg states is at least three orders of magnitude bigger than the dipolar matrix element in the two other cases.

The implication of neglecting these matrix elements is that we will have a block structure like the one in figure 3.2.

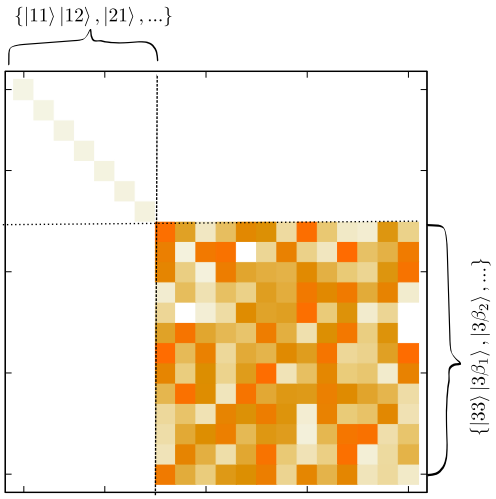

Figure 3.2: Structure of H_A: the section corresponding to pair states where both states are not Rydberg states is diagonal

This in turn means that states on the second block will be mixed, whereas the states on first block will not. The basis after the first approximation is:

$$\{|11\rangle\,,|12\rangle\,,|13\rangle\,,|21\rangle\,,|22\rangle\,,|23\rangle\,,|31\rangle\,,|32\rangle\}\cup\{|\xi_L(R)\rangle\}_{i=1}^{N}$$

where $\{|\xi_L(R)\rangle\}_{i=1}^{N}$ is the set of eigenvectors resulting from diagonalising the non-diagonal part of H_A. In particular $|\xi_3(R)\rangle$ will denote the eigenvector that tends to $|33\rangle$ when $R\to\infty$.

Second approximation

In figure 3.3, the potential for 60s60s is plotted. The y axis scale is GHz, which is the scale of the energy separation between nerby Rydberg states.

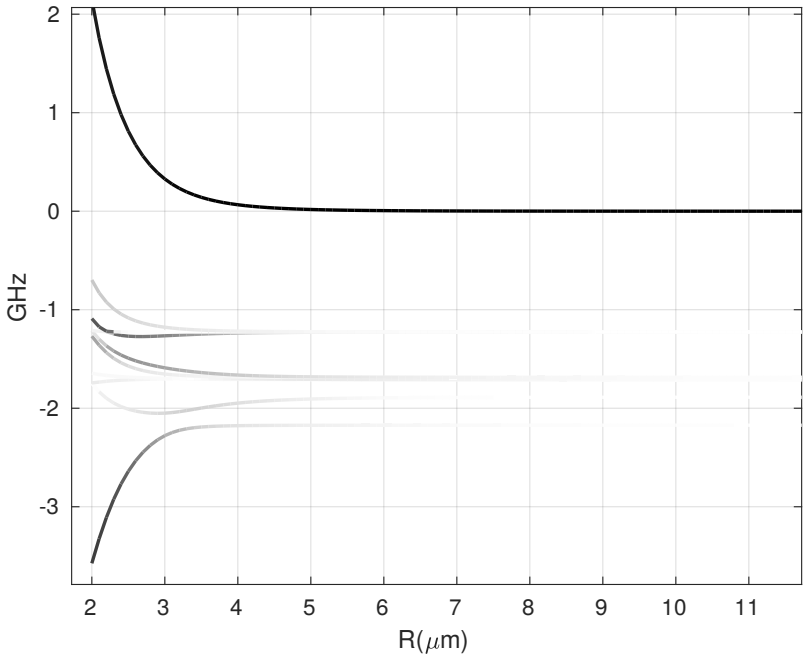

Figure 3.3: The dark curve corresponds to the potential for 60s60s. Lighter curves represent the energy curves for other eigenstates.

We can see that, as long as the atoms are sufficiently far apart ($R \geq 4\mu m$), the detuning induced by interaction is not even appreciable in the GHz scale. This implies that for most of the plotted region we can be certain that levels don't come closer due to the interaction. In other words, if we are in the region $R \geq 4\mu m$, then the only state with a double Rydberg excitation that can be excited with the scheme of lasers in figure 3.1 is $|\xi_3(R)\rangle$.

So, as long as $R \geq 4\mu m$, the basis needed to describe the system reduces to

$$\{|11\rangle, |12\rangle, |13\rangle, |21\rangle, |22\rangle, |23\rangle, |31\rangle, |32\rangle, |\xi_3(R)\rangle\} \tag{3.5}$$

Validity of second approximation

In order to test the validity of reducing the basis to the 9 elements listed before, we perform a analysis of the probability of finding a pair of atoms closer than $4\mu m$ on a cloud.

We will think that each component of the position of each atom follows a gaussian distribution of the form:

$$P(x_i) = \frac{1}{\sqrt{2\pi\sigma^2}} e^{-\frac{x_i^2}{2\sigma^2}}$$

If we have N atoms within the cloud, then we have $\frac{N(N-1)}{2}$ different pairs of atoms and distances between pairs. These distances have the distribution:

$$P_d(d) = \int_{-\infty}^{\infty} dx_1 ... \int_{-\infty}^{\infty} dz_2 \delta(\sqrt{(x_1-x_2)^2+(y_1-y_2)^2+(z_1-z_2)^2} - d) \prod_{\substack{i=1,2 \\ \chi=x,y,z}} P(\chi_i)$$

In order to do this integral we change to the variables $x_r = x_1 - x_2$ and $x = x_1 + x_2$ for each component. Writing explicitly each $P(\chi_i)$ and taking into account that for each transformation we have $J = \frac{1}{2}$ we get

$$P_d(d) = \frac{1}{(4\pi\sigma^2)^3} \int_{-\infty}^{\infty} dx_r \int_{-\infty}^{\infty} dx ... \delta(\sqrt{x_r^2+y_r^2+z_r^2} - d) e^{-\frac{x_r^2+x^2+y_r^2+y^2+z_r^2+z^2}{4\sigma^2}}$$

the ... mean that identically integrals are performed for y and z. The integrals on x, y and z are gaussians and can be done trivially. We then have

$$P_d(d) = \frac{1}{(2\pi^{3/2}\sigma)^3} \int_{-\infty}^{\infty} dx_r ... \delta(\sqrt{x_r^2+y_r^2+z_r^2} - d) e^{-\frac{x_r^2+y_r^2+z_r^2}{4\sigma^2}}$$

Next we change to spherical coordinates

$$\begin{aligned} P_d(d) &= \frac{1}{(2\pi^{3/2}\sigma)^3} \int_0^{2\pi} d\phi \int_0^{\pi} d\theta \sin\theta \int_0^{\infty} R^2 dR \delta(R-d) e^{-\frac{R^2}{4\sigma^2}} \\ &= \frac{1}{2\sqrt{\pi}\sigma^3} d^2 e^{-\frac{d^2}{4\sigma^2}} \end{aligned} \tag{3.6}$$

In figure 3.4 we plot the histogram obtained from a cloud of 10^4 atoms generated with gaussian distributions for each coordinate, the distribution (3.6). We observe that the average is above the limit set for the approximation to be valid.

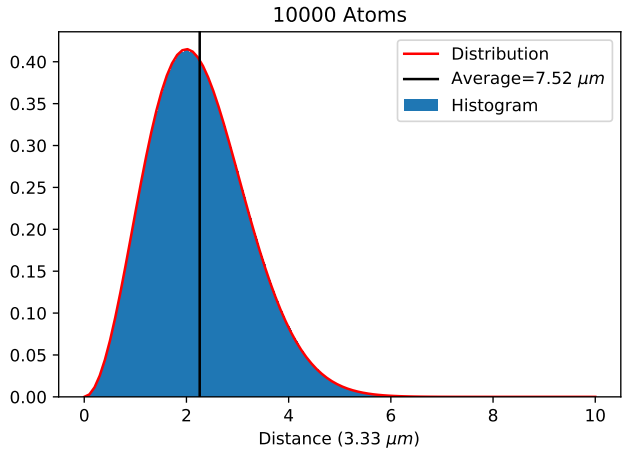

Figure 3.4: Distribution of the separation between atoms in the cloud.

Using the distribution we find that around 13% of the pairs of atoms have $R \leq 4\mu m$. From this we conclude that , at least for the case where 33=60s60s, the approximation is reasonable. This could become false if instead of 60s60s we have states with bigger principal quantum numbers.

Taking the second approximatio to be valid, the basis for our problem is (3.5). In particular, the expansion of $|\xi_{33}\rangle$ in terms of the pairs of Rydberg states is writen as:

$$\begin{aligned} |\xi_{33}\rangle &= \sum_{\alpha\beta} C_{\alpha\beta}(R)\,|\alpha\beta\rangle \\ &= C_{33}\,|33\rangle + \sum_{ij} C_{ij}\,|p_i p_j\rangle \end{aligned} \tag{3.7}$$

Note that, except for the state 33, we have included in the expansion states with a p-state on each atom. The absence of states with s or d states is justified by looking at the figure (3.5): the principal coefficients at all ranges from R correspond to p-p states.

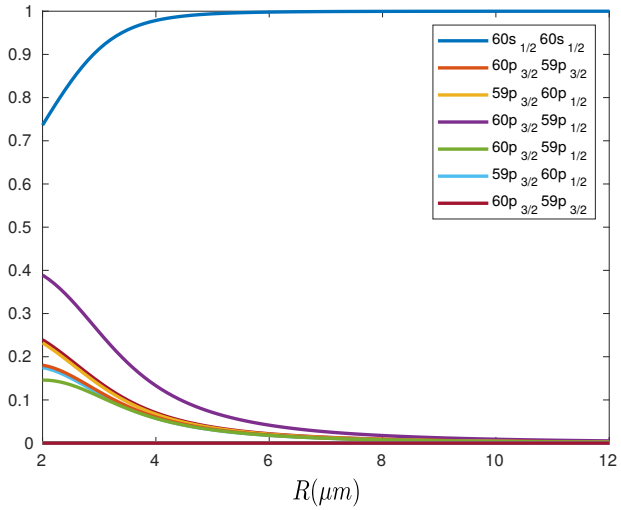

Figure 3.5: Principal composition coefficients of the state $|\xi_{33}(R)\rangle$ vs R. The principal component corresponds to the state $60s_{1/2}60s_{1/2}$, as expected

We expect this behavior also when 33=ns-ms. This is since p-p states directly couple to 33 through H_{dd}. s-s, d-d and s-d states couple only to second order, so their contribution is weaker.

Hamiltonian in the coupled basis

Writing hamiltonian (3.1) in the coupled basis (3.5) only requires us to work out the term describing the coupling to the blue laser $(-(\vec{d_1}+\vec{d_2})\cdot\vec{E}_L)$. This can be done by inserting two identities on each side of the term. Defining $\vec{d} \equiv \langle 2|\vec{d_i}|3\rangle \equiv \langle 3|\vec{d_i}|2\rangle$, the matrix elements that appear on the expansion and have to do with $|\xi_{33}\rangle$ are:

- $\langle ij|\vec{d_1}+\vec{d_2}|\xi_{33}\rangle = 0$ if $ij = 12, 21, 13, 22, 31$
- $\langle ij|\vec{d_1}+\vec{d_2}|\xi_{33}\rangle = C_{33}\vec{d}$ if $ij = 32, 23$
- $\langle \xi_{33}|\vec{d_1}+\vec{d_2}|\xi_{33}\rangle = 2\mathrm{Re}\sum_{\alpha\beta} C_{33}C^*_{\alpha\beta}\langle \alpha\beta|\vec{d_1}+\vec{d_2}|33\rangle \equiv \vec{\delta}$

Using this, we can write the hamiltonian (3.1) as:

$$H = \sum_L E_L |L\rangle \langle L| + \sum_m \hbar g(x_m) \left(a\sigma_{12}^{(m)} e^{i\omega_c t} + a^\dagger \sigma_{21}^{(m)} e^{-i\omega_c t} \right)$$
$$+ \hbar \left(\alpha^* a^\dagger e^{-i\omega_c t} + \alpha a e^{i\omega_c t} \right) + \frac{\hbar\Omega}{2} (|12\rangle \langle 13| + |21\rangle \langle 31| + |22\rangle \langle 23| + |22\rangle \langle 32|$$
$$+ C_{33} |23\rangle \langle \xi_{33}| + C_{33} |32\rangle \langle \xi_{33}| + \text{h.c}) + \delta' |\xi_{33}\rangle \langle \xi_{33}| \tag{3.8}$$

Note that the above hamiltonian is in terms of $|\xi_{33}\rangle$ and not $|33\rangle$. If we expand $|ij\rangle \langle \xi_{33}|$ to first order we obtain:

$$|ij\rangle \langle \xi_{33}| \simeq C_{33} |ij\rangle \langle 33|$$

and

$$|\xi_{33}\rangle \langle \xi_{33}| \simeq C_{33}^2 |33\rangle \langle 33|$$

so

$$H = \sum_L E_L |L\rangle \langle L| + \sum_m \hbar g(x_m) \left(a\sigma_{12}^{(m)} e^{i\omega_c t} + a_c^\dagger \sigma_{21}^{(m)} e^{-i\omega_c t} \right)$$
$$+ \hbar \left(\alpha^* a_c^\dagger e^{-i\omega_c t} + \alpha a_c e^{i\omega_c t} \right) + \frac{\hbar\Omega}{2} ((|12\rangle \langle 13| + |21\rangle \langle 31| + |22\rangle \langle 23| + |22\rangle \langle 32|$$
$$+ C_{33}^2 |23\rangle \langle 33| + C_{33}^2 |32\rangle \langle 33|) e^{i\omega_L t} + \text{h.c}) + \delta' |33\rangle \langle 33| \tag{3.9}$$

On the rotating frame defined by (where $E_1 = \hbar\omega_1$ is the energy of $|1\rangle$)

$$H_0 = \hbar \begin{pmatrix} \omega_1 & 0 & 0 \\ 0 & \omega_1 + \omega_c & 0 \\ 0 & 0 & \omega_1 + \omega_c + \omega_L \end{pmatrix} \otimes \mathbb{I}$$
$$+ \mathbb{I} \otimes \hbar \begin{pmatrix} \omega_1 & 0 & 0 \\ 0 & \omega_1 + \omega_c & 0 \\ 0 & 0 & \omega_1 + \omega_c + \omega_L \end{pmatrix}$$

the hamiltonian is

$$
\begin{aligned}
\bar{H} &= e^{\frac{iH_0t}{\hbar}} H e^{\frac{-iH_0t}{\hbar}} \\
&= \Delta_c \left|12\right\rangle \left\langle 12\right| + \Delta_c \left|21\right\rangle \left\langle 21\right| + (\Delta_c + \Delta_L) \left|13\right\rangle \left\langle 13\right| + (\Delta_c + \Delta_L) \left|31\right\rangle \left\langle 31\right| \\
&+ 2\Delta_c \left|22\right\rangle \left\langle 22\right| + (2\Delta_c + \Delta_L) \left|23\right\rangle \left\langle 23\right| + (2\Delta_c + \Delta_L) \left|32\right\rangle \left\langle 32\right| + (2\Delta_c + 2\Delta_L + \Delta) \left|33\right\rangle \left\langle 33\right| \\
&+ \sum_m \hbar g(x_m) \left(a\sigma_{12}^{(m)} + a_c^\dagger \sigma_{21}^{(m)} \right) \\
&+ \hbar \left(\alpha^* a_c^\dagger + \alpha a_c \right) + \frac{\hbar\Omega}{2} (\left|12\right\rangle \left\langle 13\right| + \left|21\right\rangle \left\langle 31\right| + \left|22\right\rangle \left\langle 23\right| + \left|22\right\rangle \left\langle 32\right| \\
&+ C_{33}^2 \left|23\right\rangle \left\langle 33\right| + C_{33}^2 \left|32\right\rangle \left\langle 33\right| + \text{h.c}) + \delta' C_{33}^2 \left|33\right\rangle \left\langle 33\right|
\end{aligned}
\tag{3.10}
$$

3.2 Selection of detunings and adiabatic elimination

Next, we choose values for the parameters that are reasonable experimentally.

The sole purpose of level $|2\rangle$ is to conect the ground state with a Rydberg states through two optical transitions. The detunings Δ_L y Δ_c are chosen so that the second level doesn't play a relevant role in the dynamics of the system when atoms are far apart. If we make $|\Delta_L|, |\Delta_c| \gg \Omega_2, g_1$ we can even adiabatically eliminate the second level. Since we also want the two-photon transition to be resonant, we parametrize the detunings as:

$$
\begin{aligned}
\Delta_c &= \frac{\delta + \bar{\Delta}}{2} \\
\Delta_L &= \frac{\delta - \bar{\Delta}}{2}
\end{aligned}
\tag{3.11}
$$

$\delta = \Delta_c + \Delta_L$ is the detuning of the two-photon transition (which should be small), and $\bar{\Delta}$ is the parameter that will determine the order of magnitude of the detunings. According to the results from adiabatic elimination we make $\delta = \frac{\Omega_2^2}{(4\bar{\Delta}^2)}$.

3.3 QuTiP Simulations

If we think that the cavity has a loss rate κ, and that the decay rates of levels $|2\rangle$ and $|3\rangle$ are γ_2 and γ_3, then the master equation that describes the system is:

$$\begin{aligned}\dot{\rho} &= -\frac{i}{\hbar}\left[H,\rho\right] + \mathcal{L}\left[\rho\right] \\ \mathcal{L}\left[\rho\right] &= \frac{\kappa}{2}\left(2a\rho a^\dagger - a^\dagger a\rho - \rho a^\dagger a\right) + \sum_m \frac{\gamma_2}{2}\left(2\sigma_{12}^{(m)}\rho\sigma_{21}^{(m)} - \sigma_{21}^{(m)}\sigma_{12}^{(m)}\rho - \rho\sigma_{21}^{(m)}\sigma_{12}^{(m)}\right) \\ &\quad + \sum_m \frac{\gamma_3}{2}\left(2\sigma_{23}^{(m)}\rho\sigma_{32}^{(m)} - \sigma_{32}^{(m)}\sigma_{23}^{(m)}\rho - \rho\sigma_{32}^{(m)}\sigma_{23}^{(m)}\right)\end{aligned} \tag{3.12}$$

The parameters left to specify are $\Omega, \bar{\Delta}, g, \kappa, \alpha,$.

- $\Omega = 2\pi \times 10$ MHz
- $\bar{\Delta} = 2\pi \times 100$ MHz
- $\kappa = 10$MHz
- The lifetime for 43S in ^{87}Rb is 42.3 μs, so that $\gamma_3 \simeq 0.02$MHz
- The lifetime for 5P in ^{87}Rb is 26.2 ns, so that $\gamma_2 \simeq 38$MHz

3.3.1 Connected correlation,populations and coherences

We ask QuTiP to calculate the stationary state for the system if the initial state is $\rho^{(0)} = |11\rangle\langle 11| \otimes |0\rangle\langle 0|$. Once we have the stationary state we calculate the populations and coherences for each atom. Besides, we calculate the connected correlation,defined as

$$\langle\sigma_{33}^{(1)}\sigma_{33}^{(2)}\rangle_C = \frac{\langle\sigma_{33}^{(1)}\sigma_{33}^{(2)}\rangle}{\langle\sigma_{33}^{(1)}\rangle\langle\sigma_{33}^{(2)}\rangle} - 1 \tag{3.13}$$

This quantity will be useful to define the blockade radius on free space: if the atoms are separated a distance such that the dipolar interaction is negligible, then the atoms are expected to be completely uncorrelated, and $\langle\sigma_{33}^{(1)}\sigma_{33}^{(2)}\rangle \simeq \langle\sigma_{33}^{(1)}\rangle\langle\sigma_{33}^{(2)}\rangle$. So $\langle\sigma_{33}^{(1)}\sigma_{33}^{(2)}\rangle_C \to 0$ when $R \to \infty$. If, on the other

hand, the atoms are close and the shift generated by dipolar interaction is important we expect to have a blockaded atom. This means we can have the two atoms simultaneously excited. Because of this, we expect that as $R \to 0$, $\langle \sigma_{33}^{(1)} \sigma_{33}^{(2)} \rangle_C \to -1$. The region of the R parameter between these two behaviors will contain the blockade radius.

In figures 3.6,3.7,3.8 and 3.9 we show the results for two different detunings $\bar{\Delta}$. The connected correlation shows the expected asymptotic behavior. If we decrease the cavity-atom coupling g two peaks appears in the uncorrelated region. In the same region, populations are coherences have minima and maxima.

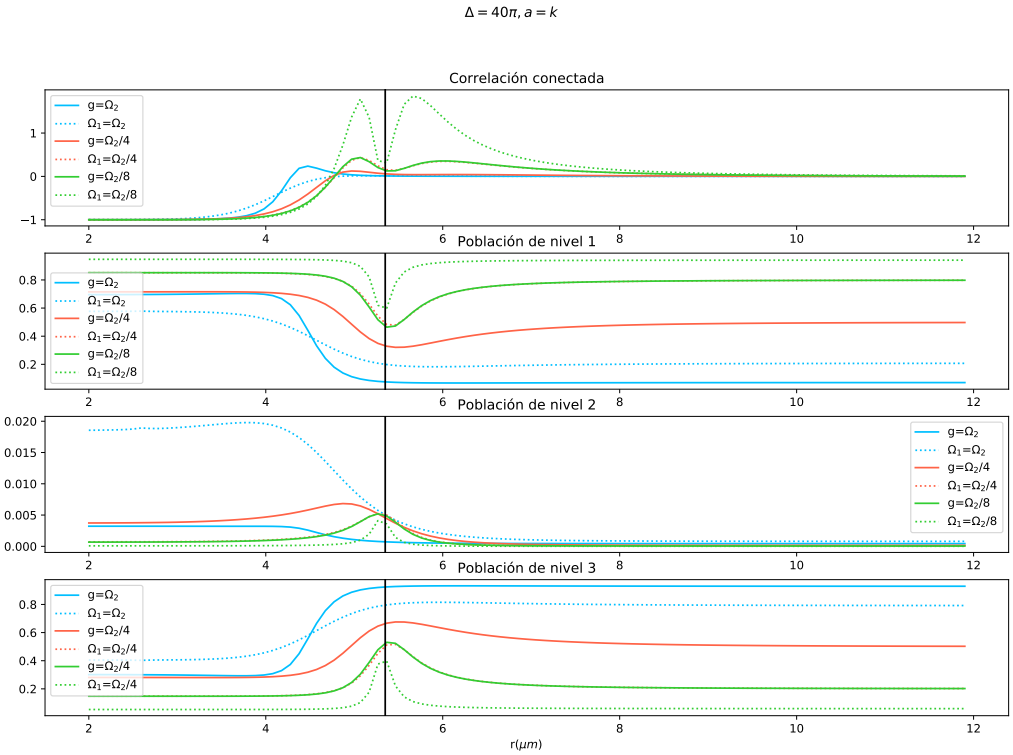

Figure 3.6: Connected correlation and populations when $\bar{\Delta} = 400\pi$MHz, $\alpha = \kappa = 10$MHz y $\Omega_2 = 40\pi$MHz

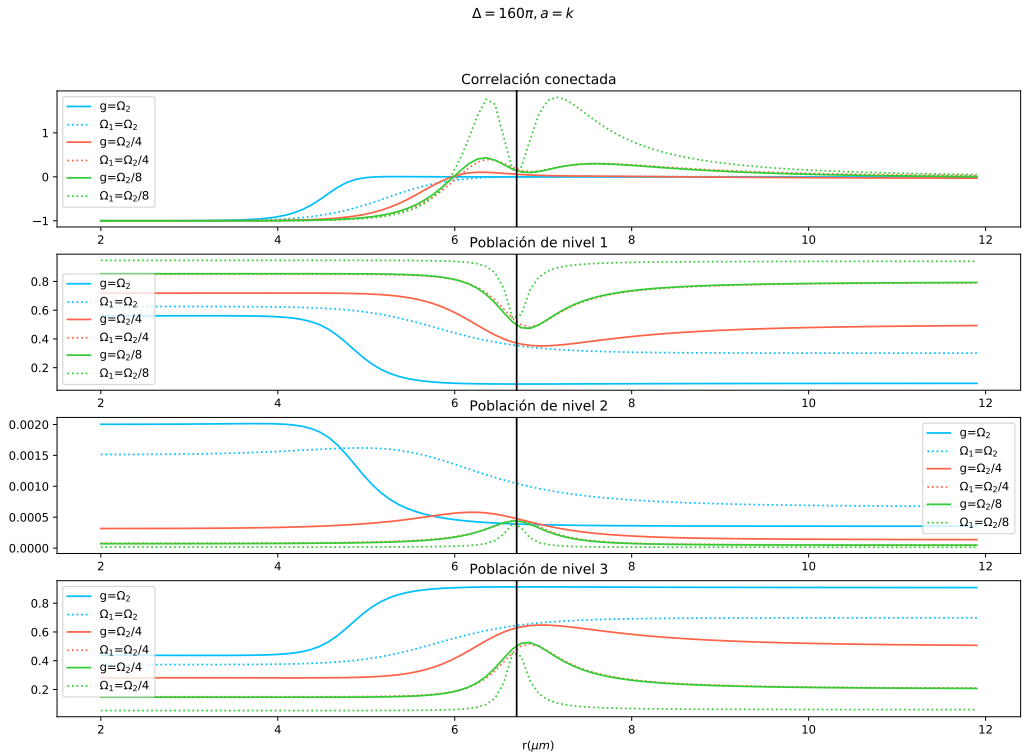

Figure 3.7: Connected correlation and populations when $\bar{\Delta} = 1600\pi\text{MHz}, \alpha = \kappa = 10\text{MHz}$ y $\Omega_2 = 40\pi\text{MHz}$

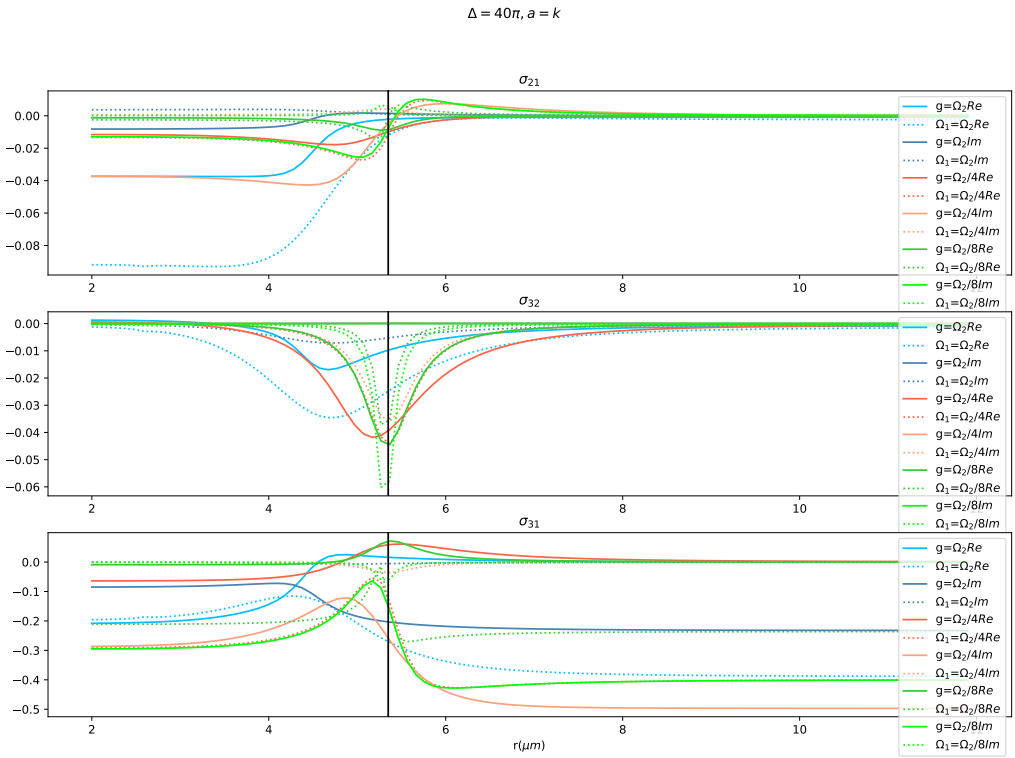

Figure 3.8: Coherences when $\bar{\Delta} = 400\pi\text{MHz}, \alpha = \kappa = 10\text{MHz}$ y $\Omega_2 = 40\pi\text{MHz}$

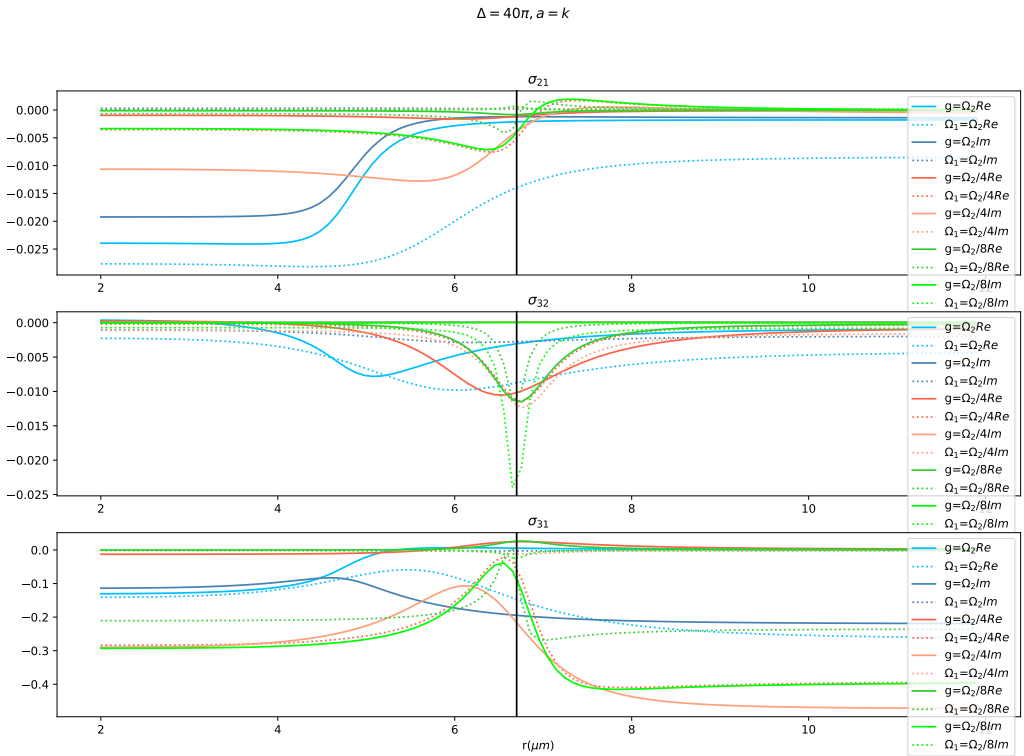

Figure 3.9: Coherences when $\bar{\Delta} = 1600\pi\text{MHz}, \alpha = \kappa = 10\text{MHz}$ y $\Omega_2 = 40\pi\text{MHz}$

Evolution equations

The evolution equation for the system are:

$$
\begin{aligned}
\dot{\sigma}_{11}^{(i)} &= ig_1(a\sigma_{21}^{(i)} - a^\dagger\sigma_{12}^{(i)}) + \gamma_2\sigma_{22}^{(i)} \\
\dot{\sigma}_{22}^{(i)} &= ig_1(a^\dagger\sigma_{12}^{(i)} - a\sigma_{21}^{(i)}) + i\frac{\Omega}{2}(\sigma_{32}^{(i)} - \sigma_{23}^{(i)}) - \gamma_2\sigma_{22}^{(i)} + \gamma_3\sigma_{33}^{(i)} \\
\dot{\sigma}_{33}^{(i)} &= i\frac{\Omega}{2}(\sigma_{23}^{(i)} - \sigma_{32}^{(i)}) - \gamma_3\sigma_{33}^{(i)} \\
\dot{\sigma}_{12}^{(i)} &= -(i\Delta_c + \frac{\gamma_2}{2})\sigma_{12}^{(i)} + ig_1a(\sigma_{22}^{(i)} - \sigma_{11}^{(i)}) - i\frac{\Omega}{2}\sigma_{13}^{(i)} \\
\dot{\sigma}_{23}^{(i)} &= -(i\Delta_L + \frac{1}{2}(\gamma_2 + \gamma_3)\sigma_{23}^{(i)}) + ig_1a^\dagger\sigma_{13}^{(i)} + i\frac{\Omega}{2}(\sigma_{33}^{(i)} - \sigma_{22}^{(i)}) - i\Delta[\sigma_{23}\sigma_{33}]_i \\
\dot{\sigma}_{13}^{(i)} &= -(\frac{\gamma_3}{2} + i(\Delta_c + \Delta_L))\sigma_{13}^{(i)} + ia\sigma_{23}^{(i)} - i\frac{\Omega}{2}\sigma_{12}^{(i)} - i\Delta[\sigma_{13}\sigma_{33}]_i \\
\dot{a} &= -ig_1(\sigma_{12}^{(1)} + \sigma_{12}^{(2)}) - i\alpha^* - \frac{\kappa}{2}a
\end{aligned}
\tag{3.14}
$$

where we have defined

$$
[\sigma_{k\ell}\sigma_{33}]_i \equiv \sigma_{k\ell}^{(i)}\sigma_{33}^{(\bar{i})}
$$

Evolution of the atomical system in free space

To check our understanding of the system and the program we compare the evolution of populations from QuTiP and the one obtained from considering the sam system without cavity. In this case the first transition is mediated by a laser with Rabi frequency Ω_1. We will compare for the two regions of parameter R we understand: when atoms are far apart and when they are blockaded.

Atoms far apart: independent Rabi oscilations

Suppouse that the detunings of the two lasers are such that we can adiabatically eliminate the second level of each atom. Once we have done the elimination, each atom is a two-level system coupled to radiation with Rabi frequency $\Omega = \frac{\Omega_1\Omega_2}{\Delta}$. Each atom couples to radiation on an independent manner. If the initial state is $|11\rangle$, the state at time t of the i-th atom is

$$
|\psi_i(t)\rangle = i\cos\left(\frac{\Omega t}{2}\right)|1_i\rangle + \sin\left(\frac{\Omega t}{2}\right)|3_i\rangle \tag{3.15}
$$

so the state of the total system is

$$|\psi(t)\rangle = |\psi_1(t)\rangle\,|\psi_2(t)\rangle \tag{3.16}$$

from the last result we can deduce that

$$\begin{aligned}
\langle\sigma_{11}^{(1)}\rangle &= \cos^4\left(\frac{\Omega t}{2}\right) + \frac{1}{4}\sin^2(\Omega t) \\
\langle\sigma_{33}^{(1)}\rangle &= \sin^4\left(\frac{\Omega t}{2}\right) + \frac{1}{4}\sin^2(\Omega t) \\
\langle\sigma_{1111}\rangle &= \cos^4\left(\frac{\Omega t}{2}\right) \\
\langle\sigma_{3333}\rangle &= \sin^4\left(\frac{\Omega t}{2}\right) \\
\langle\sigma_{WW}\rangle &= \frac{1}{2}\sin^2(\Omega t)
\end{aligned} \tag{3.17}$$

where $\sigma_{11}^{(1)}, \langle\sigma_{33}^{(1)}\rangle$ are the populations of levels 1 and 3 of atom 1, σ_{1111} is the population of state $|11\rangle$, σ_{3333} is the population of state $|33\rangle$ and σ_{WW} is the population of the state $|W\rangle = \frac{1}{\sqrt{2}}(|13\rangle + |31\rangle)$.

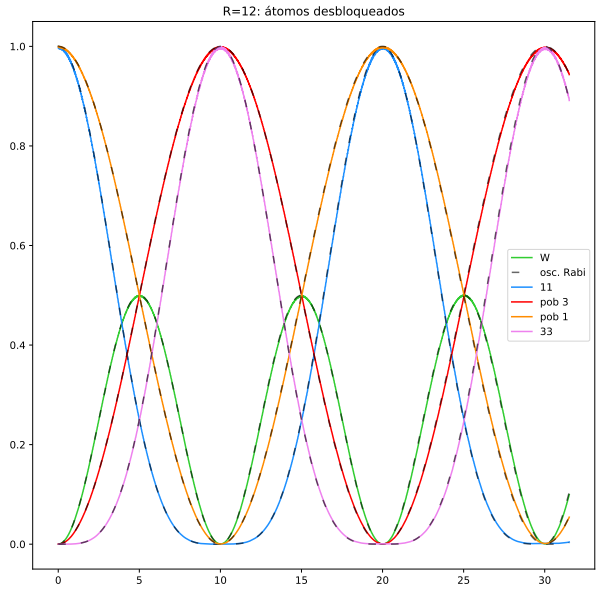

Figure 3.10: Comparison between the QuTiP population evolution (colorful lines) and the results (3.17) in gray lines

Blockaded atoms:Rabi oscilations of a superatom

When atoms are close to one another we expect the system to behave as a superatom. That is, we expect oscilations from state $|11\rangle$ to state $|W\rangle$ with an increased Rabi frequency $\sqrt{2}\Omega$. If the initial state of the system is $|11\rangle$, then the state at time t will be:

$$|\psi\rangle = i\cos\left(\frac{\Omega t}{\sqrt{2}}\right)|11\rangle + \sin\left(\frac{\Omega t}{\sqrt{2}}\right)|W\rangle \tag{3.18}$$

From this we can obtain that the populations are:

$$\begin{aligned}
\langle \sigma_{11}^{(1)} \rangle &= \cos^2\left(\frac{\Omega t}{\sqrt{2}}\right) + \frac{1}{2}\sin^2\left(\frac{\Omega t}{\sqrt{2}}\right) \\
\langle \sigma_{33}^{(1)} \rangle &= \frac{1}{2}\sin^2\left(\frac{\Omega t}{\sqrt{2}}\right) \\
\langle \sigma_{1111} \rangle &= \cos^2\left(\frac{\Omega t}{\sqrt{2}}\right) \\
\langle \sigma_{3333} \rangle &= 0 \\
\langle \sigma_{WW} \rangle &= \sin^2\left(\frac{\Omega t}{\sqrt{2}}\right)
\end{aligned} \tag{3.19}$$

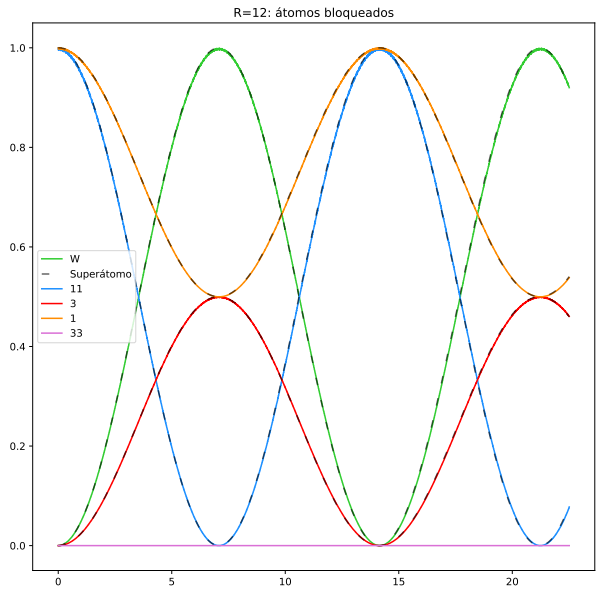

Figure 3.11: omparison between the QuTiP population evolution (colorful lines) and the results (3.19) in gray lines.

Chapter 4

Apendix A: Matrix Numerov Method

Our objective is to solve the Schrödinger equation in one dimension. This can be done with the usual Numerov method, where one guesses the energy and then integrates the equation from the initial boundary to the final one. The guess of the energy is refinated until one is able to fullfill both boundary conditions. This method can become inefficient if one is interested in solving the Schrödinger equation for multiple energies, as is our case.

An atractive alternative to this procedure is the matrix Numerov method [6]. This method consists in discretizing the wavefunction and converting the problem to a matrix eigenvalue problem. Let the interval where we want to solve for the wavefunctions be $[x_I, x_F]$. We pick an equispaciated lattice of points $\{x_i\}$ belonging to this interval and describe a wavefunction with a vector whose components are the values of the wavefunction at these points. The operators that form the Schrödinger equation become matrices in this approach.

The Schrödinger equation in 1D has the form

$$\psi''(x) = -2m\frac{(E - V(x))}{\hbar^2}\psi(x)$$

By expanding $\psi''(x)$ using second-order finite differences, we are left with the expresion

$$\frac{-\hbar^2}{2m}B^{-1}A\vec{\psi} + V\vec{\psi} = E\vec{\psi} \tag{4.1}$$

where $\vec{\psi} \equiv (\psi(x_I), \psi(x_1), ..., \psi(x_F))$, $V = \text{diag}(V(x_I), ...V(x_F))$, and A and B are simple matrices whose expresions can be found in [6]. The important observation to make is that 4.1 is an eigenvalue problem. By diagonalizing the matrix on the left side we obtain a set of eigenvectors and eigenvalues. Interestingly, by increasing the number of points on the lattice we can archieve more precision in the obtained wavefunctions and get more eigenenergies and wavefunctions.

4.1 Solution of the radial Schrödinger equation

The equation we are interested in solving is

$$\frac{d^2u}{dr^2} + 2\left(E - V_M - \frac{\ell(\ell+1)}{2r^2}\right)u = 0 \tag{4.2}$$

where V_M is the Marinescu potential. In particular, we are interested in solving the problem for high-energy states. There are two main reasons why it is not straightforward to solve this equation with the method we just review

- We expect the wavefunctions who are solution of the equation (4.2) to have a similar behavior to the radial hydrogen wavefunctions. In figure 4.1, near the origin, we can observe the hydrogen radial wavefunction for a high energy state. This wavefunction has an increasing density of oscilations as we approach to the origin. Thus, in order to solve the problem efficiently, it would be desirable to have a lattice that mimics this behavior: more points as we approach to the origin.

- We have a singularity at $r = 0$. This can be fixed by restricting the interval where we solve the equation to $[r_{\min}, r_{\max}]$

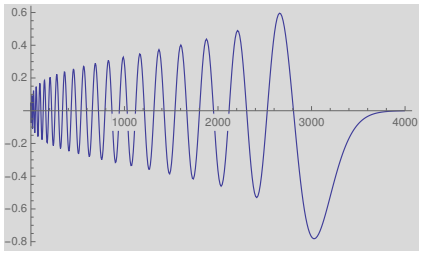

Figure 4.1: Hydrogen radial wavefunction with n=40. Image taken from [14]

The first point is fixed by considering an equispaciated lattice $\{s_i\}$ and making a new non-equispaciated lattice $\{r_i\}$ with $r_i = s_i^2$. The lattice $\{r_i\}$ will then have a bigger density of points near the origin. Next, we first make the change variable $r = s^2$ in equation (4.2), so we obtain the equation we should solve for the equispaciated lattice s.

In order to obtain an equation with the form $\psi''(s) = f(s)\psi(s)$ and apply the method on last section directly, we make $u(r) = J(s(r))\psi(s(r))$ [14]. J will be used to eliminate factors that contain the first derivative of ψ. The second derivative in (4.2) is then:

$$\frac{d^2u}{dr^2} = \frac{\psi(s)J''(s)}{4s^2} - \frac{\psi(s)J'(s)}{4s^3} + \left(\frac{J'(s)}{2s^2} - \frac{J(s)}{4s^3}\right)\chi'(s) + \frac{J(s)\psi''(s)}{4s^2} \quad (4.3)$$

So we need $\frac{J'(s)}{2s^2} - \frac{J(s)}{4s^3} = 0$. The solution to that equation is $J(s) = \sqrt{s}$. So, making $u(s) = \sqrt{s}\psi(s)$, the equation that $\psi(s)$ satisfies is:

$$\psi''(s) = 8s^2\left(\frac{3}{32s^4} + V_{\text{eff}}\left(s^2\right) - E\right)\psi(s) \quad (4.4)$$

with $V_{\text{eff}}(s^2) = V(s^2) + \frac{\ell(\ell+1)}{2s^4}$. The equation 4.4 has the form $\psi''(s) = f(s)\psi(s)$, so we can apply the method described in the first section.

4.2 Example: Hydrogen atom

As a check, we apply the method to the case of hydrogen atom (making $V(r) = \frac{1}{r}$) and compare the results with the exact wavefunctions.

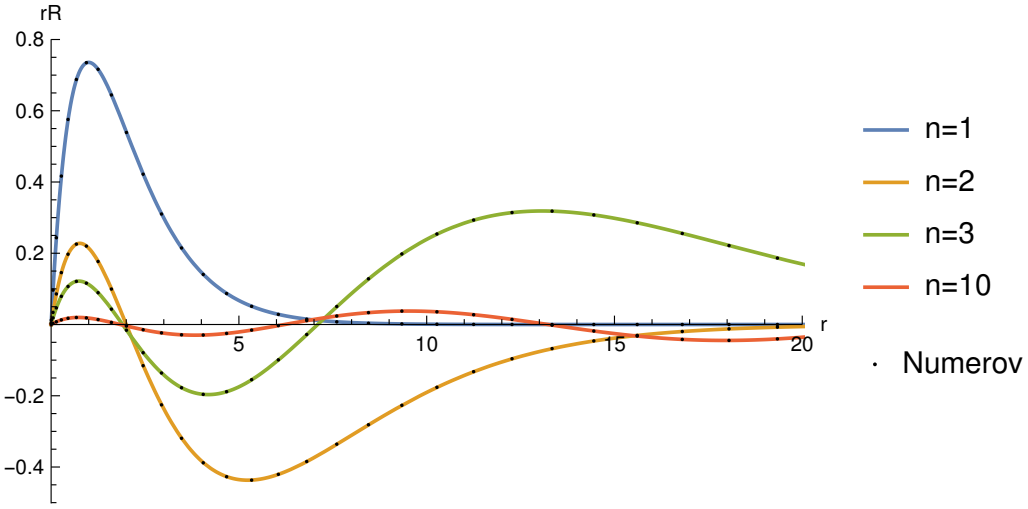

Figure 4.2: Comparison between Numerov and analytical wavefunctions.

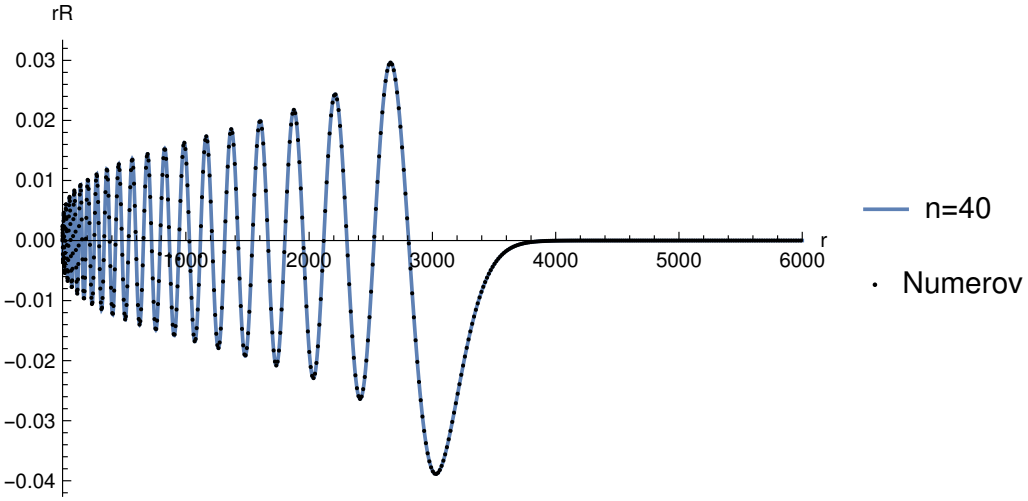

Figure 4.3: Comparison between Numerov and analytical wavefunctions.

Bibliography

[1] C. Fabret, P. Goy and S. Haroche, **Millimetre resonances in Na Rydberg levels detected by field ionization : quantum defects and Stark-effect studies**, 1977. J. Phys. B: Atom. Molec. Phys., 10, 6.

[2] G. Nogues, A. Rauschenbeutel, S. Osnaghi, M. Brune, J. Raimond and S. Haroche,**Seeing a single photon without destroying it**,1990. Nature 400, 239.

[3] B. Höglund and P. G. Mezger,**Hydrogen Emission Line $n_{110} \rightarrow n_{109}$: Detection at 5009 Megahertz in Galactic H II Regions**, 1965.Science 150, 3694.

[4] R. Löw, H. Weimer, J. Nipper, J.Balewski1,B. Butscher, H. P. Büchler and T. Pfau,**An experimental and theoretical guide to strongly interacting Rydberg gases**, 2012. J. Phys. B: At. Mol. Opt. Phys. 45, 113001.

[5] M. Marinescu,H. Sadeghpour and A.Dalgarno,**Dispersion coefficients for alkali-metal dimers**, 1994 Phys. Rev. A 49 9828.

[6] M. Pillai, J. Goglio and T. Walker, **Matrix Numerov method for solving Schrödingers equation**, Am. J. Phys. 80, 1017 (2012)

[7] J. Raimond,G. Vitrant and S. Haroche, **Spectral line broadening due to the interaction between very excited atoms: 'the dense Rydberg gas'**, 1981. J. Phys. B: At. Mol. Phys. 14 L655

[8] N. Sibalic and C.S. Adams, **Rydberg Physics**, 2018. IOP Publishing Ltd.

[9] N. Sibalic, j .D.Pritchard, C.S.Adams and K.J.Weatherill, **ARC: An open-source library for calculating properties of alkali Rydberg atoms**, 2017,Comp. Phys. Comm., 220, 319.

[10] S. Svanberg, P. Tsekeris and W. Happer, **Hyperfine-Structure Studies of Highly Excited D and F Levels in Alkali Atoms Using a cw Tunable Dye Laser**, 1973. Phys. Rev. Lett., 30,18.

[11] E. Urban, T. Johnson, T. Henage, L. Isenhower, D. Yavuz, T. Walker and M. Saffman, **Observation of Rydberg blockade between two atoms**, 2009. Nature Physics 5, 110114

[12] S.Weber, C. Tresp, H. Menke, A. Urvoy, O. Firstenberg, H. Bchler and S. Hofferberth,**Calculation of Rydberg interaction potentials**, 2017 J. Phys. B: At. Mol. Opt. Phys. 50 133001

[13] W. Li, I. Mourachko, M. W. Noel, and T. F. Gallagher, **Millimeter-wave spectroscopy of cold Rb Rydberg atoms in a magneto-optical trap: Quantum defects of the ns, np, and nd series**, Phys. Rev. A,2003 67, 052502

[14] http://www.physics.wisc.edu/ tgwalker/NumerovExamples/

n7.To qualitatively understand the RydbergRydberg interaction, consider that another Rydberg atom produces a low frequency field ? proportional to the induced Rydberg dipole which scales as n2. Consequently, when considering only the dipoledipole term of the interaction Hamiltonian, we obtain a van-der-Waals type interaction scaling as ?a n211. CHECK Nonlinear quantum optics mediated by Rydberg interactions